UNIVERSITÄT
HEIDELBERG
ZUKUNFT
SEIT 1386

Theoretical Biophysics
A Computational Approach
Concepts, Models, Methods and Algorithms
Phase Transitions

Dieter W. Heermann

May 17, 2020

Heidelberg University

Table of Contents

Introduction

Introduction I

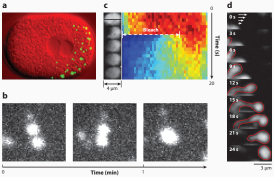

Liquid droplets in cytoplasm

Source:DOI:10.1146/annurev-cellbio-100913-013325

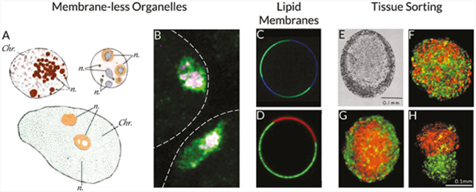

Formation of membraneless organelles

Source:

DOI:10.1039/C8SM02285B

Phase Diagrams

Phase Diagrams I

The phase diagram shows the areas of existence of the phases of a substance depending on thermodynamic parameters. The simplest phase diagram is obtained for a symmetrical binary mixture or for the Ising model with up-down symmetry. A phase diagram for this case is shown in the Figure 2. A similar, albeit inverted diagram is obtained when molecularly uniform polymers are dissolved in a low-molecular solvent.

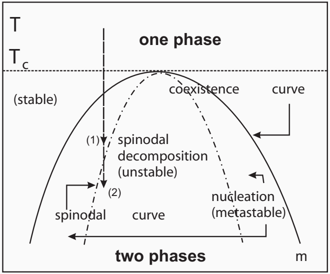

Figure 1: Simple phase diagram for a symmetric mixture of two components.

Phase Diagrams II

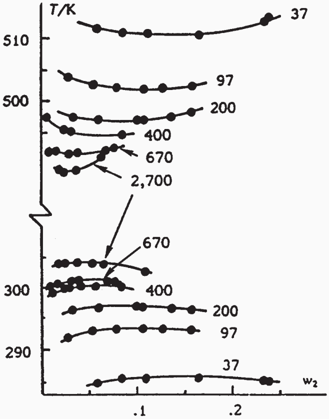

Figure 2: High and low temperature demixing curves of a system of cyclohexan/polystyrene. The x-axis shows the fraction for polystyrene.

Phase Diagrams III

Let us consider carbon dioxide as another example. Here the triple point at 5.81 bar is far above atmospheric pressure. The associated temperature is -57C. Carbon dioxide is not liquid under normal pressure, but only under increased pressure.

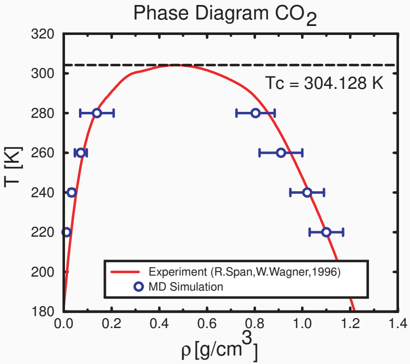

Figure 3: Phasendiagram for a CO_2 mixture.

Phase Diagrams IV

Another typical phase diagram is shown in Figure 4. Two phases can coexist at the phase boundaries in the $p-T$-diagram. At the triple point ($p_{\text{tr}}, T_{\text{tr}}$) three phases coexist, and at the critical point (p_c, T_c) the difference between the liquid and gaseous phases disappears.

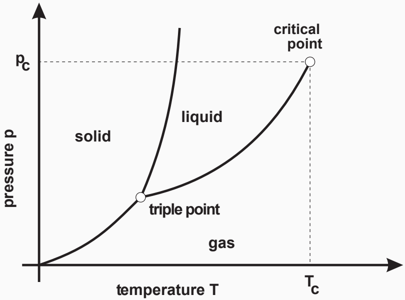

Figure 4: Typical phase diagram with a critical point (p_c, T_c) and triple point.

Phase Diagrams V

Let us consider the equilibrium between a phase i and a phase j. The coexistence curve in the $p - T$ diagram is

$$p = p_{ij}(T)\ . \tag{1}$$

Since particles can be exchanged between the two phases, the chemical potentials are the same

$$\mu_i\left(T, p_{ij}(T)\right) = \mu_j\left(T, p_{ij}(T)\right). \tag{2}$$

With the transition of ΔN_{ij} particles from phase i into phase j there will be a "latent heat" ΔQ_{ij}

$$\begin{aligned} \Delta Q_{ij} &= T\left\{-\left(\frac{\partial S_i}{\partial N}\right)_{T,p} + \left(\frac{\partial S_j}{\partial N}\right)_{T,p}\right\}\Delta N_{ij} \\ &= T\left\{\left(\frac{\partial \mu_i}{\partial T}\right)_p - \left(\frac{\partial \mu_j}{\partial T}\right)_p\right\}\Delta N_{ij} \qquad , \end{aligned} \tag{3}$$

Phase Diagrams VI

where for the pressure (1) was used. The second equation follows from the first in that entropy and chemical potential appear as the first derivatives of free enthalpy. Differentiation of (2) along the phase boundary provides

$$\left(\frac{\partial \mu_i}{\partial T}\right)_p - \left(\frac{\partial \mu_j}{\partial T}\right)_p = -\left\{\left(\frac{\partial \mu_i}{\partial p}\right)_T - \left(\frac{\partial \mu_j}{\partial p}\right)_T\right\}\frac{dp_{ij}(T)}{dT} \quad . \tag{4}$$

The derivations of the chemical potential after the pressure can, however, be computed from the Duhem Gibbs relation ($SdT - Vdp + Nd\mu = 0$)

$$\left(\frac{\partial \mu_i}{\partial p}\right)_T = \frac{V_i}{N_i} \quad . \tag{5}$$

With this we obtain the **Clausius-Clapeyron** equation

$$\Delta Q_{ij} = -T\frac{dp_{ij}(T)}{dT}\Delta V_{ij} \ , \tag{6}$$

that relates the latent heat ΔQ_{ij}, volume change ΔV_{ij} and slope of the phase boundary in the $(p - T)$-diagram.

Phase Diagrams VII

In the gas space above a liquid, the saturation pressure (vapor pressure) depends on T, which depends on T (vapor pressure curve). The above equation can be used to approximate the vapor pressure curve (sublimation curve).

We neglect the volume of the liquid (solid phase) compared to that of the gas phase and assume that only the binding energy is important for the energy of the liquid

$$E_{\mathrm{f}} = -\epsilon N \qquad\qquad \epsilon > 0\ . \tag{7}$$

The gas phase is considered the ideal gas of non-interacting particles. Both assumptions do not apply near the critical point, but are otherwise fulfilled relatively well.

The latent heat can thus be calculated by integrating the first law

$$\begin{aligned} \Delta Q_{fg} &= \Delta E_g - \Delta E_f + p_{fg}\left\{\delta V_g - \Delta V_f\right\} \\ &\approx \left\{\frac{3}{2}k_B T + \epsilon + k_B T\right\}\Delta N. \end{aligned} \tag{8}$$

For the vapor pressure curve you get (6)

Phase Diagrams VIII

$$\frac{dp(T)}{dT} = \frac{\frac{5}{2}k_B T + \epsilon}{k_B T^2} p(T) \qquad , \tag{9}$$

and hence

$$p(T) = A\, T^{\frac{5}{2}}\, e^{-\epsilon/k_B T}. \tag{10}$$

From (7) we get $\mu_{\mathrm{fl}} = -\epsilon$. Since the chemical potentials of the liquid and gaseous phases must be the same, and since (10) must also satisfy the equations of state of the gas, the initially undetermined integration constant is A is given by (10).

The binding energy can thus be determined experimentally, at least approximately, from the vapor pressure curve.

Phase Diagrams Example

For a binary mixture of A and B atoms with concentrations c_A and c_B, the two-phase coexistence line is calculated in a molecular field approximation, which provides a result similar to the Ising model

MAPLE

```
restart;
cb:= 1 - ca;
m:= ca - cb;
t:=m/(ln((1+m)/(1-m)));
plot(t,ca=0..1.0,color=black);
```

Phase Diagrams I

After this discussion of simple phase diagrams, it is beyond the scope of an introduction to theoretical biophysics to talk about complicated situations. Nevertheless, it should not be concealed that there are considerably more complex situations with many substances or combinations of substances. An example is the phase diagram for that of the polystyrene and CO_2 system in Figure 5.

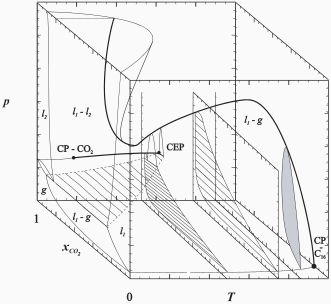

Figure 5: Phasendiagramm für das System Polystrol-CO_2

Phase Diagrams II

After this general discussion about phase boundaries, let's take a closer look at the two-phase area. In Figure 2 we separated the area into the thermodynamically stable states from the thermodynamically metastable or thermodynamically unstable states by the coexistence curve. Let us now consider the case in which a system is brought from a thermodynamically stable state into one which is unstable or metastable. This is indicated in Figure 6. This so-called quench can be done in different ways. It can be done by quickly changing the temperature or by switching on a magnetic field.

Phase Diagrams III

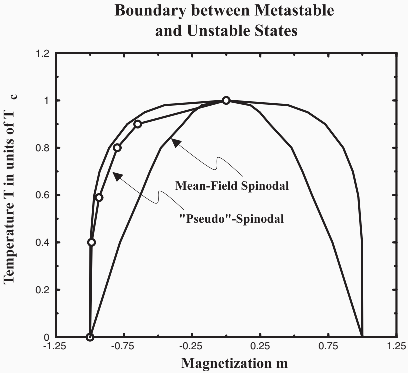

Figure 6: Generic phase diagram of a system with two components.

Phase Diagrams IV

First, let's consider the case where the quench is made in the area between the coexistence curve and the spinodal. We had marked this area as metastable because the free energy there does not have an absolute minimum. There is only a relative minimum with a certain barrier height that separates the metastable minimum value from that of the absolute minimum. It is found experimentally that this metastable state is reduced by fluctuations. These fluctuations are droplets. We can try to understand this degradation of the metastable state by the potty through the nucleation theory. This theory goes back to Becker and Döring and is essentially a rate theory. In the simplest formulation, we assume that there are no concentration fluctuations in the system initially. The system is homogeneous with a certain free energy. This free energy now corresponds to the metastable state. The system is not in an equilibrium state with regard to its parameters and is now trying to get into the equilibrium state through fluctuations in concentration.

Let n_s be the number of droplets of size s, R_s be the rate of condensation of atoms for droplets of size s and R'_s the rate of evaporation. The rate

J_s (per unit volume), with which the droplets grow from size s zu $s+1$ is given by

$$J_s = R_s n_s - R'_{s+1} n_{s+1} \tag{11}$$

Phase Diagrams V

From this we get the continuity equation

$$\frac{\partial n_s}{\partial t} = J_{s-1} - J_s \quad s \geq 2 \tag{12}$$

In the stationary state we have

$$J := J_1 = J_2 = \ldots \tag{13}$$

J is called the **nucleation rate**. $s = 0$ is the source and every droplet that is larger than the critical droplet size (s^*) continues to grow. Hence

$$J = \left(\int \frac{ds}{n_s R_s} \right)^{-1} \qquad . \tag{14}$$

Phase Diagrams VI

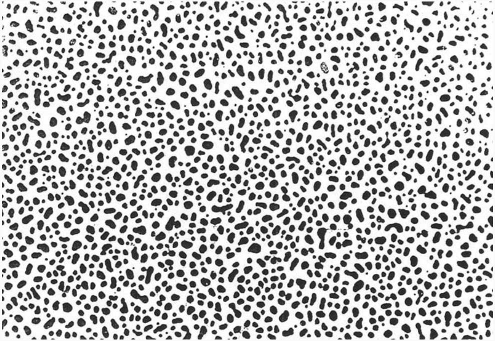

Figure 7: Droplets in a system

Phase Diagrams VII

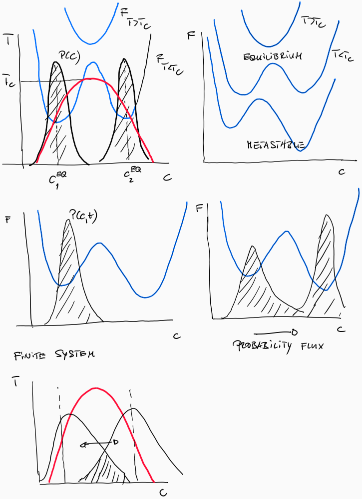

Figure 8: Free energy and probability distributions

Phase Diagrams VIII

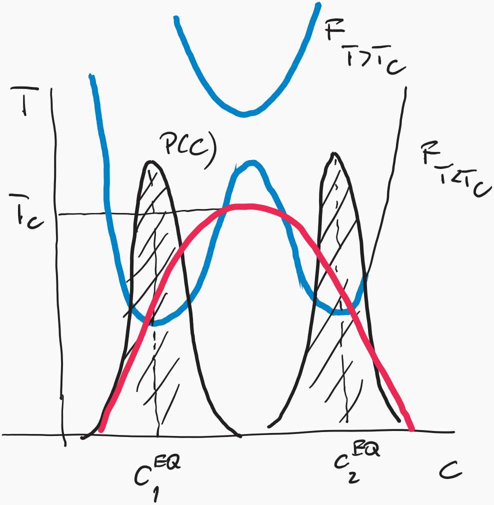

Figure 9: Free energy and probability distributions

Phase Diagrams IX

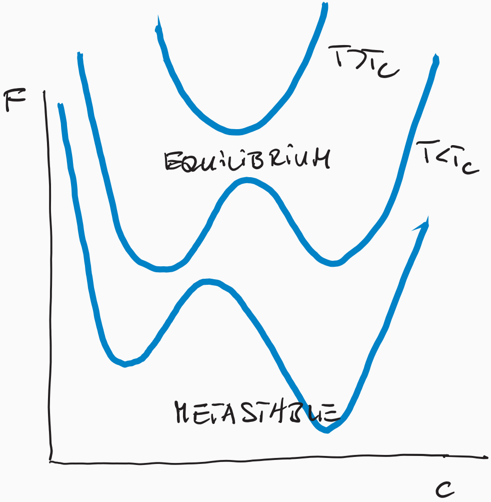

Figure 10: Free energy and probability distributions

Phase Diagrams X

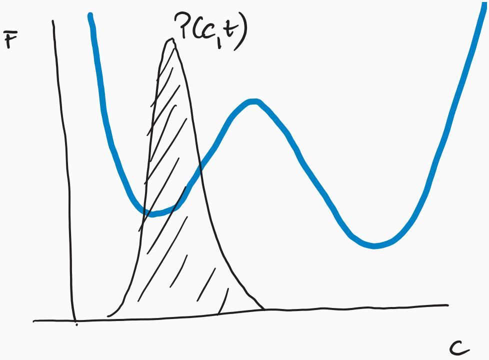

Figure 11: Free energy and probability distributions

Phase Diagrams XI

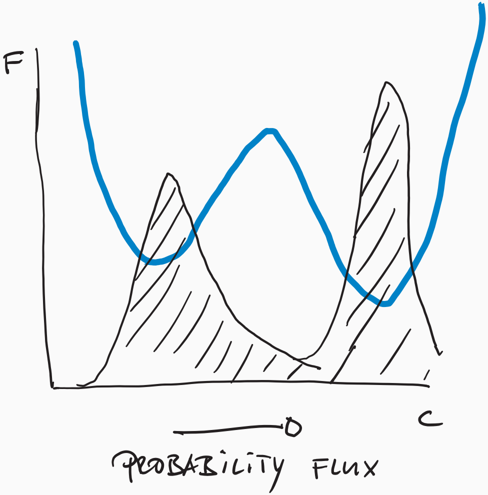

Figure 12: Free energy and probability distributions

Phase Diagrams XII

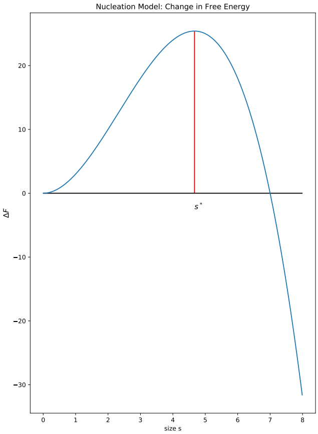

Figure 13: Nucleation barrier modelled by the competition between a surface and a volume term.

Phase Diagrams XIII

Let us assume

$$n_s \propto e^{-\Delta F/k_B T} \; . \tag{15}$$

with the implicit assumption that the droplets do not interact. We model the change in free energy as the competition between a volume and a surface term (c.f. Figure **??**)

$$\Delta F = s^2\Gamma - s^3 h \tag{16}$$

where Γ is the surface tension and h is an abbreviation for a gas/liquid system of $h = \Delta\rho\delta\mu$, the change in density and the change in chemical potential. The change in free energy has a maximum at

$$\Delta F' = 2s\Gamma - 3s^2 h = 0 \tag{17}$$

hence at

Phase Diagrams XIV

$$s^* = \frac{2\Gamma}{3h} \tag{18}$$

Droplets below the maximum size s^* will predominantly shrink and those above s^* predominantly grow. The number of droplets s^* determine the rate of conversion of the metastable state. Hence

$$J \propto n_s^* \propto e^{-4\frac{\Gamma^3}{27h^2}} \tag{19}$$

in units of the Ising model.

Phase Diagrams XV

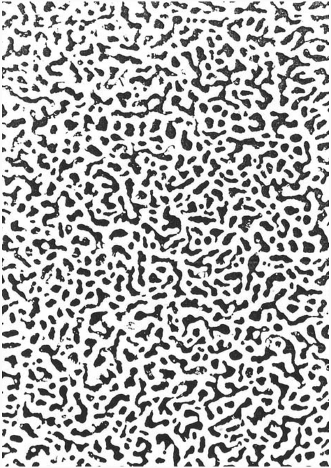

Figure 14: The figure shows a snap shop of system undergoing spinodal decomposition.

Phase Diagrams XVI

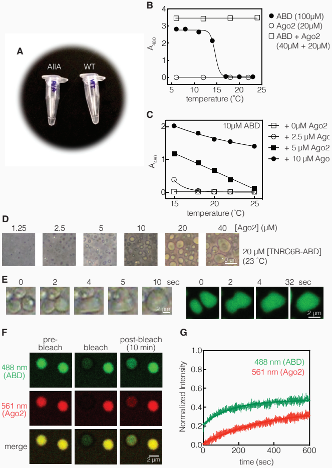

Figure 15: Ago2 Drives Phase Separation of the TNRC6B-ABD. Image taken from: Phase Transitions in the Assembly and Function of Human miRISC [1]

Critical Phenomena I

Critical points can be found not only in the liquid-gaseous phase transition, for example in the van der Waals equation, but also in magnets, order-disorder phase transitions, superconductivity and other phase transitions. The behavior of the respective systems in the vicinity of the critical point is very similar.

Table 1: Critical temperature and critical pressure for some gases.

Material	T_c (C)	P_c (at)
helium (He)	-267,95	2,34
carbon dioxid (CO_2)	75,27	31,0
water vapor (H_2O)	374,2	225,5
air	-140,73	38,5

Critical Phenomena II

We first examine the surroundings of the critical point in the van der Waals theory. At the critical point T_c, p_c, V_c we have

$$\begin{aligned} \left(\frac{\partial p}{\partial V}\right)_{T_c,N} &= -\left(\frac{\partial^2 F}{\partial V^2}\right)_{T_c,N} = 0 \\ \left(\frac{\partial^2 p}{\partial V^2}\right)_{T_c,N} &= -\left(\frac{\partial^3 F}{\partial V^3}\right)_{T_c,N} = 0. \end{aligned} \tag{20}$$

We expand the free energy (**??**) in powers of

$$\Delta\rho = \rho - \rho_c = \frac{N}{V} - \frac{N}{V_c} \tag{21}$$

and get

$$\begin{aligned} F \quad = \quad & F_{\mathrm{vdW}}(T, N, V_c) - p_0(T)\,(V - V_c) + \tfrac{1}{2}\,a\,N\,(T - T_c)\,\Delta\rho^2 \\ & + \tfrac{1}{3}\,b\,N(T - T_c)\,\Delta\rho^3 + \tfrac{1}{4}\,u\,N\,\Delta\rho^4. \end{aligned} \tag{22}$$

Critical Phenomena III

The various parameters, in particular a, b and u, are determined by the virial coefficients b_0 and b_1. We are interested in $|T - T_c| \sim \Delta\rho^2$. Hence the contributions proportional of b and u can be dropped and we get the isotherm

$$p(T, \rho) = p_0(T) + \rho_c^2 \left\{ a\,(T - T_c)\,\Delta\rho + u\,\Delta\rho^3 \right\} \tag{23}$$

and the special critical isotherm

$$p(T_c, \rho) = p_c + \rho_c^2\, u\, \Delta\rho^3. \tag{24}$$

For the compressibility at the critical density for $T > T_c$ we get

$$\kappa^{-1}(T, \rho_c) = -V\,\frac{\partial p}{\partial V} = \rho\,\frac{\partial p}{\partial \rho} = a\,\rho_c^3\,(T - T_c) \tag{25}$$

$\kappa(T, \rho_c)$ diverges at the critical point.

To calculate the properties for $T < T_c$ we need the Maxwell- or double tangent construction. Neglecting b in (22), $F + (V - V_c)\,p_0$ is an even function of $\Delta\rho$ and the density at coexistence is given by the minima of $F + (V - V_c)\,p_0$

Critical Phenomena IV

$$(T - T_c)\, a\, \Delta\rho + u\, \Delta\rho^3 = 0\,; \qquad \Delta\rho = \pm\sqrt{(T_c - T)\, a/u}. \tag{26}$$

The compressibility at the coexistence curve is

$$\begin{aligned} \kappa^{-1} &= \rho_c^3 \left\{(T - T_c)\, a + 3\, u\, \Delta\rho^3\right\} \\ &= 2\, a\, \rho_c^3\, (T_c - T). \end{aligned} \tag{27}$$

The compressibility below T_c is finite, however, diverges as one approaches the critical point.

The specific heat is given by

$$C_V = -T \left(\frac{\partial^2 F}{\partial T^2}\right). \tag{28}$$

Critical Phenomena V

For $T > T_c$ and $V = V_c$ only $F_{\mathrm{vdW}}(T, N, V_c)$ contributes to (22). For $T < T_c$ we need to take into account $\Delta\rho$ according to (26). With this we get

$$\begin{aligned} C_{V_c} &= C_{\mathrm{reg}}(T) = -T\left(\frac{\partial^2 F_{\mathrm{vdW}}(T)}{\partial T^2}\right) && T > T_c \\ &= C_{\mathrm{reg}}(T) + \tfrac{1}{2}\, N\, \frac{a^2}{u}\, T && T < T_c . \end{aligned} \tag{29}$$

The specific heat has a discontinuity at the critical point.

The free energy of a magnet in the vicinity of the critical point (Curie point) can be developed accordingly

$$F(T, N, M) = F_0(T, N) + \tfrac{1}{2}\, a\,(T - T_c)\, N\,(M/N)^2 + \tfrac{1}{4}\, u\, N\,(M/N)^4 + \cdots . \tag{30}$$

M is the magnetization. Odd terms do not occur due to the symmetry. The previous calculations can be transferred directly to the magnet, where $\Delta\rho$ is substituted by M/N, $p - p_c$ and the magnetic field B and κ_T by the isothermal susceptibility χ_T.

In addition to the van der Waals equation of state, Berthelot proposed another molecular field-like equation of state

$$P = \frac{8T}{3v-1} - \frac{3}{Tv^2} \tag{31}$$

We would like to calculate the critical exponents.

MAPLE

```
> restart;
> P:=(v,T)->8*T/(3*v-1)-3/(T*v^2);
> p1:=(nu,epsilon)=P(1+nu,1+epsilon)-1;
> aux:=series(8*(1+epsilon)/(2+3*nu)-3/(1+epsilon)/(1+nu)^2-1,
          nu=0,4):aux;
> aux1:=(epsilon)->3+4*epsilon-3/(1+epsilon)+(-6-6*epsilon+
    6/(1+epsilon))*nu
   +(-9*1/(1+epsilon)+9+9*epsilon)*nu^2 +(12*1/(1+epsilon)-
   27/2-27/2*epsilon)*nu^3;
> aux2:=series(aux1(epsilon),epsilon=0,2);
```

We now get a simplified equation of state with the critical point $\epsilon = 0$. Since t curve is symmetrical, the gas and liquid components must be the same: $v_g = -v_l = v$. From this we can get the critical exponent β .

MAPLE

```
> p:=(nu,epsilon)->-3/2*nu^3+(7-12*nu)*epsilon;
> d1:=(nu,epsilon)->subs(y=nu,diff(p(y,epsilon),y)): d1(nu,epsilon);
> solve(p(v,epsilon)= p(-v,epsilon),v);
```

Hence $\beta = 1/2$ and for the exponent δ we get

MAPLE

```
> P1:=(rho,T)->8*T*rho/(3-rho)-3*rho^2/T:
> P1(1+xi,1);
> series(8*(1+xi)/(2-xi)-3*(1+xi)^2,xi=0);
```

the value $\delta = 3$.

Correlation Functions

Correlation Functions I

To better understand what is happening near a critical point, we examine the behavior of the correlation function. We use the so-called average or **molecular field** approximation. Let $\hat{n}(r)$ be the density at r and $\rho = \langle \hat{n}(r) \rangle$ the average density. Then

$$\begin{aligned} \langle \hat{n}(r)\hat{n}(r') \rangle^c &= \langle \hat{n}(r)\hat{n}(r') \rangle - \rho^2 \\ &= \sum_{ij} \langle \delta(r - r_i)\delta(r' - r_j) \rangle - \rho^2 = \rho\delta(r - r') + g(r - r'). \end{aligned} \tag{32}$$

We saw that the isothermal compressibility is given by

$$\begin{aligned} \kappa_T &= \frac{1}{k_B T \rho^2} \int \langle \hat{n}(r)\hat{n}(0) \rangle^c d^3 r \\ &= \frac{1}{k_B T \rho} + \frac{1}{k_B T \rho^2} \int g(r) d^3 r \, . \end{aligned} \tag{33}$$

Since the compressibility diverges at the critical point, but the density ρ remains finite, the range of the correlations must diverge.

Correlation Functions II

We consider a gas in a weak spatially inhomogeneous field, which is given by a potential $\varphi(r)$. This is the Hamilton function

$$H_\varphi = H + \sum_i \varphi(r_i) = \sum_i \frac{p_i^2}{2m} + \frac{1}{2}\sum_{ij} W(r_i - r_j) + \sum_i \varphi(r_i) \tag{34}$$

and the density on the presence of a field

$$\langle \hat{n}(r)\rangle_\varphi = \sum_i \frac{\mathrm{Tr}\,\delta(r - r_i)\, e^{-\beta(H + \sum_j \varphi(r_j))}}{\mathrm{Tr}\, e^{-\beta(H + \sum_j \varphi(r_j))}} \; . \tag{35}$$

For a small external potential one get to first order

$$\begin{aligned} \delta\langle \hat{n}(r)\rangle_\varphi = \langle \hat{n}(r)\rangle_\varphi - \rho \quad &\approx \quad -\beta \sum_j \left\{ \langle \delta(r - r_i) \sum_j \varphi(r_j)\rangle - \rho \sum_j \langle \varphi(r_j)\rangle \right\} \\ &= \quad -\beta\rho \left\{ \varphi(r) + \int' g(r - r')\varphi(r') d^3 r \right\} \; . \end{aligned} \tag{36}$$

Correlation Functions III

We want to take the effect of the interaction $W(r_i - r_j)$ at least approximately into account. In addition to the potential $\varphi(r_i)$, the selected particle i is also affected by the potential for interaction with the other particles

$$\varphi_{\mathrm{eff}}(r_i) = \varphi(r_i) + \sum_j W(r_i - r_j) \; . \tag{37}$$

The approximation now consists in replacing this potential by an averaged potential, averaging over the positions of the particles j. Only the deviations from the homogeneous density $\delta\langle \hat{n}(r)\rangle_\varphi$ need to be taken into account, since the interaction in the case of homogeneous density has already been included in the van der Waals equation. So that is

$$\bar{\varphi}_{\mathrm{eff}}(r) = \varphi(r) + \int W(r - r')\delta\langle n(r')\rangle_\varphi d^3r' \; . \tag{38}$$

In this approximation, the density reads

$$\delta\langle n(r)\rangle_\varphi = -\beta\rho\bar{\varphi}_{\mathrm{eff}}(r) \; . \tag{39}$$

Correlation Functions IV

Substituting this with (38) in (36) we get

$$\begin{aligned}
\delta\langle n(r)\rangle_\varphi &= -\beta\rho\varphi(r) - \beta\rho\int g(r-r')\varphi(r')d^3r' \\
&= -\beta\rho\varphi(r) + \beta^2\rho^2\int W(r-r')\varphi(r')d^3r' \\
&\quad +\beta^2\rho^2\int W(r-r')g(r'-'')\varphi(r'')d^3r'd^3r'' \,. \qquad (40)
\end{aligned}$$

However, this must apply to any external potential $\varphi(r)$, and one obtains an integral equation for the correlation function:

$$\begin{aligned}
g(r-r') &= -\beta\rho W(r-r') \\
&\quad -\beta\rho\int W(r-r'')g(r''-r')d^3r'' \,. \qquad (41)
\end{aligned}$$

Assume the range of interaction to be ξ_0. We are interested in distances $|r-r'| \gg \xi_0$ and expand $g(r''-r')$ around $r-r'$

Correlation Functions V

$$
\begin{aligned}
g(r''-r') &= g(r-r') + \sum_\alpha (r''_\alpha - r_\alpha)\frac{\partial}{\partial r_\alpha} g(r-r') \\
&\quad + \frac{1}{2}\sum_{\alpha\beta}(r''_\alpha - r_\alpha)(r''_\beta - r_\beta)\frac{\partial^2}{\partial r_\alpha \partial r_\beta} g(r-r') + \dots \qquad (42)
\end{aligned}
$$

We can insert this into (41) obtaining this following integrals

$$
\begin{aligned}
\int W(\bar{r}) d^3\bar{r} &= -W_0 = -2b_1 k_B \\
\int \bar{r}_\alpha W(\bar{r}) d^3\bar{r} &= 0 \\
\int \bar{r}_\alpha \bar{r}_\beta W(\bar{r}) d^3\bar{r} &= -\delta_{\alpha\beta} W_2 = -\delta_{\alpha\beta}\xi_0^2 W_0 \ . \qquad (43)
\end{aligned}
$$

This now gives the differential equation for the correlation function

$$
g(r) = -\beta\rho W(r) + \beta\rho W_0 g(r) + \frac{1}{2}\beta\rho W_2 \Delta g(r) \ , \qquad (44)
$$

Correlation Functions VI

where we need to use $\Delta = \partial^2/\partial_r^2 + \frac{2}{r}\partial/\partial_r$ This equation has for large distances $r \gg \xi_0$ the solution

$$g(r) = g_0 \, \frac{1}{r} \, e^{-r/\xi} \tag{45}$$

with the correlation length

$$\xi^2 = \frac{\xi_0^2}{\frac{T}{2\rho b_{\mathbf{1}}} - 1} \; . \tag{46}$$

With the van der Waals equation (**??**) we get for the isothermal compressibility

$$\kappa_T = -\frac{1}{V(\partial p/\partial V)} = \frac{(V/N)^2 - b_0^2}{2\, k_B b_1} \, \frac{1}{\frac{T}{2\rho b_{\mathbf{1}}} - (1 - \rho b_o)^2} \; . \tag{47}$$

It should be noted that in the previous derivation, the strongly repulsive portion of the interaction was not taken into account with sufficient accuracy, and therefore the divergence of the correlation length does not coincide with the divergence of compressibility. A treatment similar to the derivation of the van der Waals equation yields instead of (46)

Correlation Functions VII

$$\xi^2 = \frac{\xi_0^2}{\frac{T}{2\rho b_1} - (1 - \rho b_0)^2} \; . \tag{48}$$

This means that the correlation length diverges precisely where in the van der Waals equation $(\partial p/\partial V)_T = 0$, hence where the compressibility diverges. This curve in the $V - T$- or $\rho - T$-diagram is known as the spinodal.

The correlation length diverges at the critical density ρ_c and for $T > T_c$ we have

$$\xi = \frac{\frac{2}{3}\xi_0}{\sqrt{(T - T_c)/T_c}} \tag{49}$$

and for $T < T_c$ along the coexistence cureve

$$\xi = \frac{\frac{1}{3}\sqrt{2}\,\xi_0}{\sqrt{(T_c - T)/T_c}} \; . \tag{50}$$

Using the results (45, 49, 50) to compute the compressibility (33) we get in the neighborhood of the critical point for $\rho = \rho_c$ and $T > T_c$

Correlation Functions VIII

$$\kappa_T = \frac{6\pi g_0}{\xi_0^2 \rho_c^2} (T - T_c)^{-1} \,, \tag{51}$$

hence the same result as in (25) with

$$g_0 = \xi_0^2 / 6\pi a \,. \tag{52}$$

We can also get an improved estimate of the specific heat from the correlation function. The starting point is the relation

$$C_p = \frac{1}{k_B T} \langle (H + pV)^2 \rangle_p^c \,. \tag{53}$$

From (22) one obtains with

$$E = F + T \frac{\partial F}{\partial T} \tag{54}$$

in the neighborhood of the critical point

$$(E + pV) - (E_c + p_c V) \simeq \frac{1}{2} V \rho_c T_c a \Delta\rho^2 + \ldots \,. \tag{55}$$

Correlation Functions IX

This suggests to use in (53) approximately

$$H + pV \simeq E_c + p_c V_c + \frac{1}{2}\rho_c T_c a \int (\hat{n}(r) - \rho_c)^2 \, d^3 r \ . \tag{56}$$

With this for $T > T_c$

$$\begin{aligned} C_p &\simeq \frac{(\rho_c T_c a)^2}{4 k_B T_c} V \int \left\{ \langle \hat{n}^2(r) \hat{n}^2(0) \rangle - \langle \hat{n}^2 \rangle^2 \right\} d^3 r \\ &\simeq \frac{(\rho_c T_c a)^2}{4 k_B T_c} V \int g^2(r) d^3 r \ . \end{aligned} \tag{57}$$

Substitute into this (45) and (49) we get

$$C_p \sim (T - T_c)^{-1/2} \ , \tag{58}$$

hence, a divergence of the specific heat at the critical point in qualitative agreement with experiments. This calculation goes beyond the previous one as it takes, at least to some degree, as fluctuations are taken into account which become particularly important especially in the vicinity of the critical point, A corresponding divergence is obtained for $T < T_c$.

Correlation Functions X

We now come back to the Markov processes and examine the correlation with regard to the time that prevails at the critical point. This requires some definitions.

Let $f = \{f(x)\}_{x \in S} \to \mathbb{R} \in L^2_\pi$ and $\mathcal{P}$ be a stationary Markov chain with stationary distribution π. Then with $\{f_t\} := \{f(X_t)\}$ we have a stationary stochastic process. We define

- $\mu_f := \langle f_t \rangle = \sum_x f(x)\pi_x$ (**average**)
- $C_{ff}(t) := \langle f_s f_{s+t} \rangle - \mu_f^2 = \sum_{x,y} f(x) \left[\pi_x \phi_{xy}^{(|t|)} - \pi_x \pi_y \right] f(y)$
  non normed auto-correlation function.
- $\phi_{ff}(t) := C_{ff}(t)/C_{ff}(0)$
  normed auto-correlation function.
- $\tau_{\mathbf{exp},f} := \lim_{t\to\infty} \sup \frac{t}{-\log|\phi_{ff}(t)|}$
  exponential auto-correlation time.
- $\tau_{\mathbf{exp}} := \sup_f \tau_{\mathbf{exp},f}$
  is the relaxation time of the slowest mode.
- $\tau_{\mathbf{int},f} := \frac{1}{2}\sum_{t=-\infty}^{\infty} \phi_{ff}(t) = \frac{1}{2} + \sum_{t1=}^{\infty} \phi_{ff}(t)$
  integral auto-correlation time.

Correlation Functions XI

Now consider a Markov process where we measure f. We make n observations, then

$$\bar{f} := \frac{1}{n} \sum_{t=1}^{n} f_t \tag{59}$$

for the variance

$$\begin{aligned} \sigma &= \frac{1}{n^2} \sum_{r,s=1}^{n} C_{ff}(r-s) && (60) \\ &= \frac{1}{n} \sum_{t=-(n-1)}^{n-1} \left(1 - \frac{|t|}{n}\right) C_{ff}(t) && (61) \\ &\approx \frac{1}{n} 2\tau_{\mathbf{int},f} C_{ff}(0) \qquad n \gg \tau \text{ where } \phi_{ff}(t) \sim e^{-|t|/\tau} \; . && (62) \end{aligned}$$

In other words, in a Monte Carlo simulation or in an experiment, the correlation of the configurations leads to a reduction in the accuracy:

Instead of n independent observations we only get $n/2\tau_{\mathbf{int},f}$.

Interpretation:

Correlation Functions XII

- $\tau_{\mathbf{exp}}$ controls the number of observations that must be neglected before starting to count a quantity
- $\tau_{\mathbf{int}}$ controls the correlation

In the thermodynamic limit we have for the relaxation time τ

$$\tau \sim \xi^z \sim (1 - T/T_c)^{-\nu z}$$

(rule: $\xi \leftrightarrow L$)

$$\Rightarrow \tau_{max} \sim L^z \ \ (T = T_c)$$

In the case of the Ising-model we get for the fluctuations of the magnetization

$$\begin{aligned} \left\langle (\delta M)^2 \right\rangle &= \frac{2\tau_{max}}{t_{obs}} \left[\left\langle M^2 \right\rangle_{T_c} - \langle |M| \rangle^2_{T_c} \right] \\ &= \frac{2\tau_{max} \chi'_{max} k_B T_c}{t_{obs} L^{\alpha}} \sim L^{z+\gamma/\nu - d} / t_{obs} \end{aligned}$$

Correlation Functions XIII

Since $L^{z+\gamma/\nu} \approx L^y$ $(d \leq 4)$ we obtain:

to increase the accuracy by a factor of 10 we need 10^y more computing time.

Correlation Functions XIV

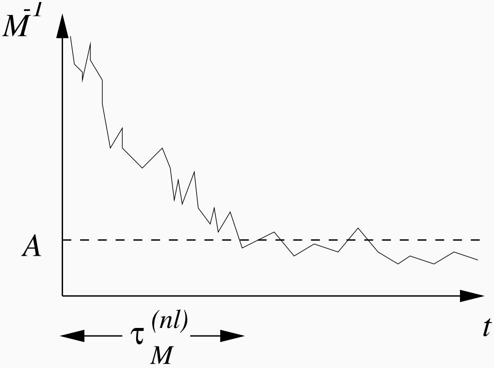

Figure 16: Non-linear relaxation time

Phase Diagrams for Macromolecules I

The *Flory-Huggins theory* of polymer solutions is based on a lattice theory. It is a mean-field theory.

Macromolecules occupy 30 percent of the volume of the cell, strongly influencing inter-molecular interactions. The density of the molecules causes like species to phase separate into different regions of the cell, leading to *macromolecular compartmentalization*.

We consider a solution of solvent molecules and polymers (see Figure 17). For simplicity we assume that the monomers of the polymer with length N have the same size as the solvent molecules. We further simplify by constraining the polymers and the solvent molecules to be on a lattice. This gives us the possibility to count the number of putting a polymer at n lattice sites with coordination number q. Let N_1 be the number of solvent molecules and N_2 be the number of polymers ($n = N_1 + NN_2$).

Phase Diagrams for Macromolecules II

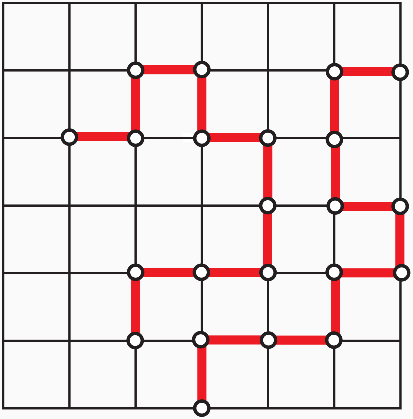

Figure 17: Lattice statistics for polymers as considered in the Flory-theory

Phase Diagrams for Macromolecules III

We assume that the polymer molecules are numbered and are placed on the lattice one after the other according to their numbers. If the number of possible ways to place the i-th monomer after the one has placed the first $i-1$ polymers is called ν_i, then the number of ways to place all the other polymers on the lattice is given by $\nu_1 \nu_2 \cdots \nu_{N_2}$. Since we cannot distinguish the polymer monomers, we must have

$$W = \frac{1}{N_2!} \prod_{i=1}^{N_2} \nu_i \tag{63}$$

for the number of configurations. Next we need to approximate ν_i. We have numbered the monomers along the chain by $1, 2, 3, ..., N$. We place the monomers on the lattice according to their ordering. The first monomer can be placed anywhere on a free lattice site. The number of possible ways to do this is

$$n - N(i-1) \; . \tag{64}$$

The second monomer needs to be placed on one of the q nearest-neighbours. We make the approximation that one can replace the probability of finding a neighbour site occupied by the polymers one has already placed by the probability one would

Phase Diagrams for Macromolecules IV

have if all other monomers were distributed randomly over the lattice. From this assumption one obtains

$$q[1 - N(i-1)/n] \tag{65}$$

for the number of ways for doing so. The third monomer needs to be placed to a nearest-neighbour site to the second monomer. One of the neighbour sites has already been taken therefore we get

$$(q-1)[1 - N(i-1)/n] \tag{66}$$

for the third monomer. If we neglect the possibility that the fourth monomer happens to be placed next to the first monomer we find the same situation for the fourth as for the third monomer. Let σ be the symmetry number of the polymer which is 2 for a polymer which is symmetric with respect to the center and 1 otherwise. Then we have

$$\nu_i = \frac{n}{\sigma} q(q-1)^{N-2} \left[1 - \frac{N(i-1)}{n}\right]^N , \tag{67}$$

Phase Diagrams for Macromolecules V

because it does not matter from which end we start laying down the polymer on the lattice. Substituting this expression into 63 we obtain

$$\begin{aligned} W &= \frac{q^{N_2}(q-1)^{N_2(N-2)}}{N_2!\sigma^{N_2}} n^{N_2} \prod_{i=1}^{N_2} \left[1 - \frac{N(i-1)}{n}\right]^N \qquad (68) \\ &= \frac{q^{N_2}(q-1)^{N_2(N-2)}}{N_2!\sigma^{N_2}} n^{-(N-1)N_2} \left[N^{N_2} \frac{(n/N)!}{(N_1/N)!}\right]^N . \qquad (69) \end{aligned}$$

The vacant sites must be filled with the solvent. Hence the whole solution is determined by the configuration of the polymers and also the entropy of the solution is given by

$$S = k_B \ln W \ . \qquad (70)$$

Inserting 69 into this we get

$$S(N_1, N_2) = N_2 k_B \ln \frac{q(q-1)^{N-2}}{\sigma e^{N-1}} - k_B \left[N_1 \ln \frac{N_1}{n} + N_2 \ln \frac{N_2}{n}\right] . \qquad (71)$$

Phase Diagrams for Macromolecules VI

We can obtain this result from a purely thermodynamic consideration. Assume that we have two species each obeying the ideal gas law ($P = nRT/V$). The gases are in a container speparted by a wall. We first expand one of the gases isothermally then the work integral we

$$W = \int_{V_1}^{V_1+V_2} PdV = n_1 RT \int_{V_1}^{V_1+V_2} V^{-1} dV \tag{72}$$

and hence

$$W = n_1 RT \ln \frac{V_1 + V_2}{V_1} \tag{73}$$

or

$$\Delta S_1 = n_1 R \ln \frac{V_1 + V_2}{V_1} \ . \tag{74}$$

For the second gas we find

$$\Delta S_2 = n_2 R \ln \frac{V_1 + V_2}{V_2} \tag{75}$$

Phase Diagrams for Macromolecules VII

So that in total we get

$$\begin{aligned}\Delta S &= \Delta S_1 + \Delta S_2 = n_1 R \ln \frac{V_1 + V_2}{V_1} + n_2 R \ln \frac{V_1 + V_2}{V_2} && (76)\\ &= -R\left(n_1 \ln \frac{V_1}{V_1 + v_2} + n_2 \ln \frac{V_2}{V_1 + v_2}\right) && (77)\end{aligned}$$

The model has some restrictions. First, there is no change of volume during mixing. Second, the entropy of mixing is entirely given by the number of rearrangements during mixing. The enthalpy of mixing is caused by interactions of different segments after the dissolution of interactions of the same type of segments.

We shall assume that there is random mixing of two polymers with no volume change. Then the combinatorial entropy of mixing is given by

$$\Delta S = -R\left(\frac{c_1}{N_1} \ln c_1 + \frac{c_2}{N_2} \ln c_2\right) \qquad (78)$$

with c_i being the volume fraction of the component i and N_i the number of monomers. Here R is the gas constant.

Phase Diagrams for Macromolecules VIII

If we assume the concept of regular solutions and assuming pair interactions then, in the framework of a mean-field theory, we obtain for the enthalpy of mixing

$$\Delta H = RT\chi c_1 c_2 \ . \tag{79}$$

Here χ is the Flory-Huggins parameter assumed not to be a function of the composition. The Flory-Huggins equation is now given by

$$\Delta F = RT\left(\frac{c_1}{N_1}\ln c_1 + \frac{c_2}{N_2}\ln c_2 + \chi c_1 c_2\right) \ . \tag{80}$$

Before we continue to examine the free energy we shall first look at model for the internal energy. Let $n = N_1 + N_2$, i.e. we consider monomers at the moment. We introduce concentrations for the cell for the two species, solvent molecules and nomomers c_i^1 and c_i^2 in the i-th cell. Since

$$c_i^2 = 1 - c_i^1 \tag{81}$$

we can introduce $c_i \equiv c_i^1$ with

Phase Diagrams for Macromolecules IX

$$N_1 = \sum_{i=1}^{n} c_i \; , \quad N_2 = \sum_{i=1}^{n} (1 - c_i) \; . \tag{82}$$

With these we can write down an interaction Hamiltonian

$$\begin{aligned} H(\{c_i\}) &= \sum_{\mu,\nu=1,2} \sum_{i,j} V_{i,j}^{\mu\nu} c_i^{\mu} c_j^{\nu} & (83) \\ &= \sum_{i,j} \left\{ V_{ij}^{11} c_i c_j + V_{ij}^{22} (1 - c_i)(1 - c_j) + 2 V_{ij}^{12} c_i (1 - c_j) \right\} \; . & (84) \end{aligned}$$

Let

$$s_i = \begin{cases} +1 & \text{if cell } i \text{ is occupied by a solvent molecule} \\ -1 & \text{if cell } i \text{ is occupied by a solute molecule} \end{cases} \tag{85}$$

then the above Hamiltonian reduces to the Ising model, if we let

Phase Diagrams for Macromolecules X

$$
\begin{aligned}
J_{ij} &\equiv V_{ij}^{12} - \frac{1}{2}(V_{ij}^{11} + V_{ij}^{22}) && (86)\\
V^{\mu\nu} &\equiv \sum_j V_{j1}^{\mu\nu} && (87)\\
J &\equiv \sum_j J_{j1} && (88)
\end{aligned}
$$

and hence

$$H(\{c_i\}) = -\frac{1}{2}\sum_{ij} J_{ij} s_i s_j + \frac{V^{11} - V^{22}}{2} + \frac{n}{2} J \, . \qquad (89)$$

It follows that the internal energy within this model is given by

$$U/n = -2J\left(c - \frac{1}{2}\right)^2 + Kc + \text{const} \qquad (90)$$

with the segment concentration

Phase Diagrams for Macromolecules XI

$$c = \frac{N \cdot N_2}{n} \ . \tag{91}$$

Phase Diagrams for Macromolecules XII

Comparison between the free energies

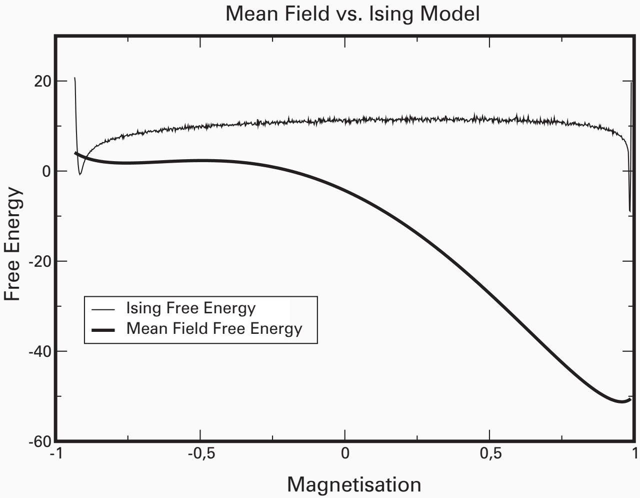

Excercises

Excercises I

Exercise 1: **van der Waals**

Consider the van der Waals equation of state

$$P = \frac{NkT}{V - Nb} - \frac{N^2 a}{V^2}$$

a) Why is the critical point given by

$$\frac{\partial P}{\partial V} = \frac{\partial^2 P}{\partial V^2} = 0 \text{ ?}$$

b) Show

$$V_c = 3Nb, \quad P_c = \frac{a}{27b^2} \quad kT_c = \frac{8a}{27b}$$

and obtain the law of corresponding states

$$p = \frac{8\tau}{3v - 1} - \frac{3}{v^2}$$

where $p = P/p_c$, $v = V/V_c$ and $\tau = T/T_c$.

c) Expand this equation up to cubic order in ϕ and t where $v = 1 + \phi$ and $\tau = 1 + t$.

d) Show for the critical exponent $\gamma = 1$ (compressibility).

e) Assume $P = -\frac{\partial F}{\partial V}|_T$ and obtain the Gibbs free energy $G = F + PV$.

Excercises II

Exercise 2: **Convexity**

A magnetic spin system is in equilibrium at temperature T. Let μ be the magnetic moment of a spin and M the average magnetization per spin hence $-\mu < M < \mu$. Let $F(M)$ be the free energy per spin for a given magnetization .

Compute the field H, for a given free energy

$$F(M) = \lambda \begin{cases} 0, & |M/\mu| \leq 1/2 \\ (|M/\mu| - 1/2)^2, & 1 \geq |M/\mu| \geq 1/2 \end{cases},$$

where λ is constant.

Exercise 3: **Two-dimensional Gas**

Consider a two-dimensional monatomic gas of N particles of size M at temperature T that only moves in the xy-plane. The volume thus becomes the area and the pressure is defined as the force per unit length.

- What is the number of molecules with velocities between v and $v + dv$? (All assumptions for the classical velocity distribution should apply.)
- Calculate the specific heat for a constant area. (Relationship between pressure, temperature, etc.)
- Calculate the specific heats at constant area (C_V) and at constant pressure (C_P)

Excercises III

- Give a formula for the number of molecules that meet a unit length (the area limit) during a time unit.

Exercise 4: **Zipper-model**

The partition function of the Zipper model ist given by

$$Z_N = \frac{1 - x^N}{1 - x}, \qquad x = G \exp(-\beta\epsilon)$$

We now want to investigate whether the system has a phase transition in relation to the order parameter $\langle s \rangle$.

- Expand $\ln Z_N$ around $x = 1 + \eta$ für $\eta \ll 1$ and then expand $\langle s \rangle$ for $\eta \ll 1$ and $N \gg 1$.
- Show that the fraction of open linker at $\eta = 0$ in the thermodynamic limit shows a jump discontinuity. Hence, show that $\frac{1}{N}\frac{d\langle s \rangle}{d\eta}$ diverges. Such an order parameter behaviour points to phase transition of first order.
- Determine T_c.

Exercise 5: **Modified van-der-Waals Gas**

The modified van der Waals gas has the following equation of state with molar volume v:

$$(p + \frac{a}{Tv^2})(v - b) = RT \quad (n > 1)$$

Excercises IV

- Determine p_c, v_c und T_c.
- Can you rewrite the equatioon of state into a universal form where the constant a and b do not feature in.
- Determine the critical exponents γ (defined by $\kappa_T \sim |\frac{T-T_c}{T_c}|^{-\gamma}$) and δ (defined by $p - p_c \sim |v - v_c|^{\delta}$ at $T = T_c$). Expand the equation of state around the critical point.

Exercise 6: **Binary Mixture**

We consider a system that consists of two types of molecules (A and B) on a cubic lattice. Each lattice site can be occupied by either a molecule of type A or B, whereby each atom can only interact with the six direct neighbors. We assume an interaction energy $-J$ between neighboring molecules of the same kind ($A - A$ and $B - B$), while pairs $A - B$ do not interact. The total number of lattice positions is N, the number of atoms of type A is N_A, the number of atoms of type B is N_B ($N = N_A + N_B$)

- Estimate the total energy of the system assuming that the atoms are randomly placed on the N lattice sites, i.e. each lattice site is occupied by a molecule A with probability N_A/N and a molecule B with probability N_B/N.
- Calculate the entropy of this mixture using the same assumption.
- In this approximation, write the free energy $F(x)$ as a function of $x = (N_A - N_B)/N$. Develop $F(x)$ up to the fourth order and show that the free energy is no longer convex below a critical temperature T_c. Specify T_c
- Plot $F(x)$ for $T < T_c$, $T = T_c$ and $T > T_c$.

Excercises V

Exercise 7: **Consider the Ginzburg-Landau Hamiltonian**

$$\beta H = \int dx \left\{ \frac{t}{2}\mathbf{m}^2 + u\mathbf{m}^4 + v\mathbf{m}^6 + \frac{\kappa}{2}(\nabla\mathbf{m})^2 - h\mathbf{m} \right\}$$

with $u > 0$ and $v = 0$. If $u < 0$, then a positive v is necessary to ensure stability.

- By sketching the free energy $F(m)$ for various values of t, show that there is a first order phase transition for $u < 0$ and $h = 0$.
- For $h = 0$ and $v > 0$ plot the phase boundary in the (u, t) plane, identifying the phases, and the order of the transition. (The special point $u = t = 0$ separating the first and second order phase boundaries is called a tricritical point).

Excercises VI

Exercise 8: **Potts Model**

Consider Potts spins $s_i = (1, 2, \ldots, q)$, interacting via the Hamiltonian

$$-\beta H = K \sum_{<i,j>} \delta_{s_i, s_j}$$

To treat this problem graphically at high temperatures, the Boltzmann weight for each bond is written as

$$\exp(K\delta_{s_i,s_j}) = C(K)[1 + T(K)g(s_i, s_j)],$$

with $g(s, s') = q\delta_{s,s'} - 1$. Find $C(K)$ and $T(K)$

a) Show that

$$\sum_{s=1}^{q} g(s, s') = 0, \quad \sum_{s=1}^{q} g(s_1, s)g(s, s_2) = qg(s_1, s_2), \quad \text{and} \quad \sum_{s,s'}^{q} g(s, s')g(s', s) = q^2($$

Excercises VII

b) An alternative is obtained by starting with

$$\exp(K\delta_{s_i,s_j}) = 1 + v(K)\delta_{s_i,s_j}$$

where $v(K) = e^K - 1$. In this case, the sum over the spins does not remove any graphs, and all choices of distributing bonds at random on the lattice is acceptable (see lecture).

i) Including a magnetic field $h\sum_i \delta_{s_i,\mathbf{1}}$, show that the partition function takes the form

$$Z(q,K,h) = \sum_{\text{all graphs}} \prod_{\text{clusters c in graph}} \left[v^{n_b^c}(q-1+e^{hn_s^c})\right]$$

where n_c^b and n_s^c are the number of bonds and sites in the cluster c. This is known as the *random cluster expansion (Fortuin-Kasteleyn expansion)*.

ii) Show that the limit $q \to 1$ describes a percolation problem, in which bonds are randomly distributed on the lattice with probability $p = v/(v+1)$.

iii) Show that in the limit $q \to 0$, only a single connected cluster contributes to leading order. The enumeration of all such clusters is known as listing *branched lattice animals*.

Bibliography

Bibliography I

References

[1] Jessica Sheu-Gruttadauria and Ian J. MacRae. Phase transitions in the assembly and function of human mirisc. *Cell*, 173(4):946–957.e16, 2018.

Index

Index I